Quantifying Noise Floor and Trace Noise in VNA Measurements for the WR-15 Waveguide Band

Aaron M. Hagerstrom*, Angela C. Stelson*, Jeffrey A. Jargon*, Christian J. Long*
*National Institute of Standards and Technology, 325 Broadway, M/S 672.01, Boulder, CO 80305 USA
Email: aaron.hagerstrom@nist.gov

2022 98th ARFTG Microwave Measurement Conference (ARFTG) | 978-1-6654-0662-8/22/$31.00 ©2022 IEEE | DOI: 10.1109/ARFTG52954.2022.9844076

***Abstract*—We present a model and measured data to assess the uncertainties in scattering-parameter measurements due to noise floor and trace noise in the receivers of a vector network analyzer operating in the WR-15 waveguide band.**

***Index Terms*—noise floor, trace noise, uncertainty, vector network analyzer, waveguide.**

I. Introduction

Scattering-parameters (S-parameters) measured by a vector network analyzer (VNA) are a fundamental microwave-frequency measurand and are part of the traceability chain for numerous quantities, including antenna factors, microwave power, and phase. At the time of this publication, an international intercomparison between national metrology institutes is currently underway to compare WR-15 calorimetric power calibrations [1]. WR-15 waveguides operate in a frequency band from 50 GHz to 75 GHz, which is of growing importance for 5G [2]. To ensure NIST traceability of S-parameter measurements, we assessed uncertainties resulting from dimensional measurements of the calibrations artifacts [3], as well as those due to noise floor and trace noise, VNA drift, VNA nonlinearity, isolation, test port cable stability, and connection repeatability [4].

In the literature, there are several existing models of noise in VNA measurements [4]–[6]. Following Ref [4], we adopt a model where noise has both multiplicative and additive components. The additive component is referred to as noise floor (NF), while the multiplicative component is referred to as trace noise (TN). The noise floor refers to signals detected by the receivers even when no RF power is incident on them. This noise is expected to be present in all measurements, and its variance is expected to be independent of the signal detected by the receivers. On the other hand, trace noise scales in proportion to the measured value of the receiver measurements. Both types of noise are dependent on the experimental setup and are reduced by smaller values of intermediate-frequency bandwidth (IF BW) or more averaging [6].

This paper is organized as follows. In Section II, we describe how we measured the trace noise and noise floor of our VNA and WR-15 extender heads. In Section III, we discuss how we model the noise, and how we extract the parameters of our model from measurements. In Section IV, we discuss how we model correlations between measurements. Finally, in Section V, we show the effect of noise on measurements of two different devices under test (DUTs).

II. Experimental procedure

To characterize the noise, we performed the following measurements. During these measurements, the lab environment was maintained at 23 °C ± 2 °C and 40 % ± 20 % relative humidity.

1) The VNA was configured to take data in continuous wave (CW) mode, with the IF BW set to 10 Hz.
2) One-port DUTs (flush shorts, offset shorts, and matched loads) were used to measure the noise floor. In these measurements, both ports were terminated to prevent crosstalk between the extender heads. The data was acquired sequentially for each port.
3) The trace noise was measured in a thru configuration with the test ports directly connected.
4) At each frequency, we acquired raw wave-parameter data at a time interval of 0.25 seconds for 400 time points.

III. Noise model and data analysis

It is convenient to represent the trace noise by its perturbations to the amplitude and phase because of its multiplicative effect on the data. The real-valued variables that represent the magnitude and phase perturbations are $\delta\mathrm{Mag}\,(w)^{(\mathrm{TN})}$ and $\delta\mathrm{Arg}\,(w)^{(\mathrm{TN})}$, respectively, where w denotes a generic wave parameter a or b. In contrast, we see that in our model, the distribution of the noise floor is centered at zero, and that a representation in terms of the real and imaginary parts of a single complex number is more appropriate. These complex numbers are denoted by $\delta w^{(\mathrm{NF})}$ Thus, the perturbed uncalibrated wave parameters are given by:

$$a'_{nm} = \left[1 + \mathrm{Mag}\,(a_{nm})^{(\mathrm{TN})}\right] \times \exp\left[j\delta\mathrm{Arg}\,(a_{nm})^{(\mathrm{TN})}\right] a_{nm} + \delta a_{nm}^{(\mathrm{NF})} \quad (1)$$

and

$$b'_{nm} = \left[1 + \mathrm{Mag}\,(b_{nm})^{(\mathrm{TN})}\right] \times \exp\left[j\delta\mathrm{Arg}\,(b_{nm})^{(\mathrm{TN})}\right] b_{nm} + \delta b_{nm}^{(\mathrm{NF})}, \quad (2)$$

where m and n refer to the port designations 1 and 2, and w_{mn} is the wave measured on port m when port n is active.

According to eqs. (1) and (2), the amplitude of the noise floor does not depend on the signal. For that reason, it was

easiest to characterize the noise floor when no signal was present. Experimentally, we attached one-port DUTs to each port of the VNA and used the wave parameters a_{mn} and b_{mn} where $m \neq n$ to evaluate the noise floor. We measured the wave parameters with each of the ports active, and with several different DUTs (a short, an open, and a load). According to the model, all these situations are equivalent, and so they can be used as independent measurements of the same physical process. Since both test ports were terminated, we expected no power to be transmitted between them in the absence of crosstalk. If crosstalk were present, it would manifest as a reproducible signal. We did no observe crosstalk, if there had been any crosstalk, it would not impact our uncertainty estimates because our noise model is based on the variance of the data irrespective of its mean (Section III).

Since trace noise is multiplicative, it is most easily detected when the signal is relatively large. From eqs. (1) and (2), the distribution of the wave parameters is expected to depend on the nominal value. To characterize the trace noise distribution in a way that is independent from the DUT, we divide measured values by their average over all measurements $\bar{w}$. Then, we compute the change in the amplitude and phase according with to

$$\delta\mathrm{Mag}\,(w) = \mathrm{Mag}\left(\frac{w}{\bar{w}} - 1\right) \tag{3}$$

and

$$\delta\mathrm{Arg}\,(w) = \mathrm{Arg}\left(\frac{w}{\bar{w}}\right). \tag{4}$$

Because trace noise only manifests when a measurable signal is present, we need to measure it using a standard where all eight of the wave parameters (a_{mn} and b_{mn} for all combinations of n and m) are expected to be non-zero. A mismatched two-port device would probably be ideal, but we did not have one available. For this reason, to characterize the trace noise we used repeated measurements of a thru standard. For these two-port measurements, there was significant power transmission between the two ports, that is $a_{mn} \neq 0$ and $b_{mn} \neq 0$. There was also a measurable reflection coefficient from both ports of the thru. Therefore, the signal was large enough that the trace noise could be detected for each of the wave parameters.

In Fig. 1, we show the measured samples of noise floor and trace noise at 60 GHz as an example. The general features of Fig. 1 do not vary as a function of frequency, but the magnitude of the noise does. In our plots of the noise floor, we see that the variance of the real and imaginary parts are approximately equal. The noise floor of the a wave is larger than the b wave by a factor of about 17. These data are uncalibrated, and the noise level may be affected by both the VNA and the extender heads. So, at this point we do not wish to speculate on the physical interpretation of this difference in the magnitude of the noise in the a and b waves.

In Fig. 1, we also plot the trace noise as determined by eqs. (3) and (4). In our plots of the trace noise, we see that trace noise is approximately of the same magnitude for the a and b waves. We also see that qualitatively, trace noise impacts

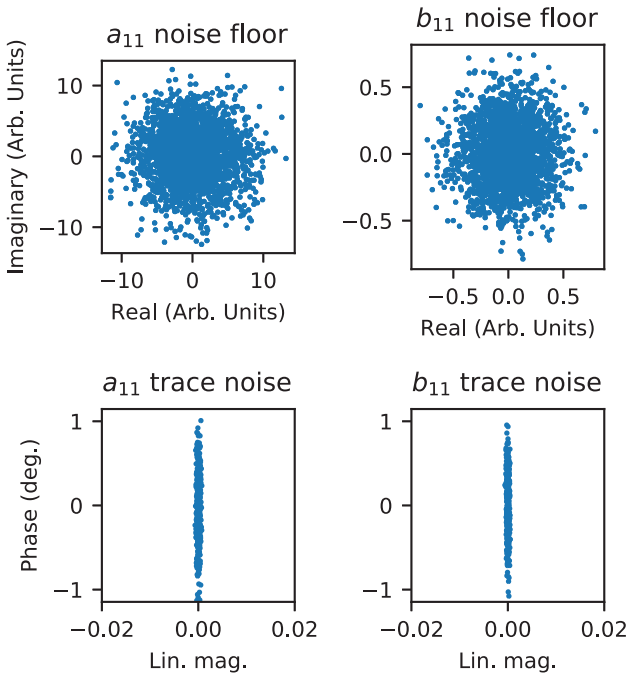

Fig. 1: Repeated measurements of the noise floor and trace noise at 60 GHz. These data are used to model the probability distribution of the noise. The scale of the noise floor data is arbitrary because the data are uncalibrated. The trace noise plots are scaled to show the relative contributions of magnitude and phase noise to wave parameters in the real-imaginary representation.

phase much more than magnitude (corresponding to a factor of about 35 in a real-imaginary representation).

We will see in Section V, trace noise has a much larger impact on measurements that the noise floor, but we cannot directly compare them in this figure because the units of trace noise and the noise floor are different.

IV. Correlations

There are two types of correlation that may be relevant to our discussion, correlations between data measured at different frequencies and correlations between the wave parameters. Correlations between frequencies can be very important when the data are Fourier-transformed into the time domain [2]. We will defer discussion of frequency correlations until the end of the section. The other type of correlation is correlation between the wave parameters. Our trace noise model is derived from measurements of all eight wave parameters. Since each of the eight wave parameters have magnitude and phase, the data have $8 \times 2 = 16$ dimensions of the data for each frequency point. In our analysis, the trace noise data was represented as a list of 16-dimensional real-valued vectors, where each vector is an independent measurement. From this set of measurements, we constructed a 16×16 sample covariance matrix. Then, we determined the eigenvalues, σ_i^2 and eigenvectors v_i of the covariance matrix.

Fig. 2 illustrates some of the correlations between the wave parameters at 60 GHz. The full 16×16 correlation matrix is hard to visualize due to the number of variables, so we picked a few representative variables. Evidently, the wave parameters measured when port 1 is active are correlated, and the wave parameters measured when port 2 is active are correlated. But the trace noise measured when port 1 is active is uncorrelated with the trace noise measured when port 2 is active. The eigenvectors associated two largest eigenvalues are shown. These eigenvectors are, scaled so that their magnitude is σ_i.

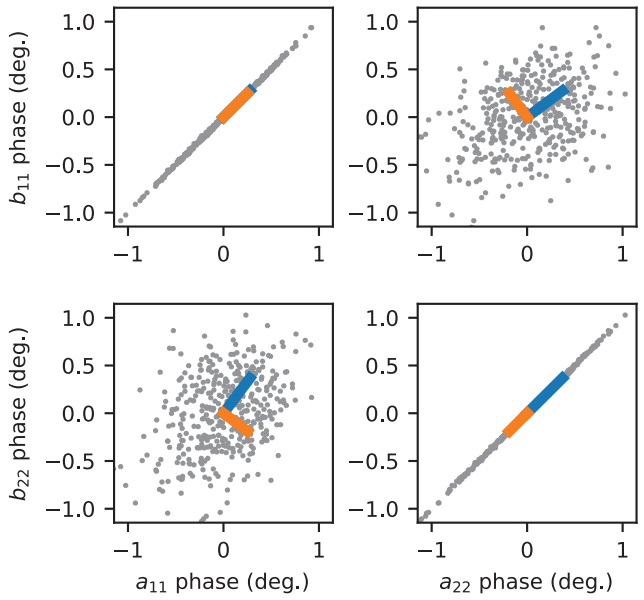

Fig. 2: Correlations in the trace noise at 60 GHz. The projections of the two largest uncertainty vectors are shown.

When we analyzed the noise floor, we took a slightly different approach. The noise floor could not be independently measured for all 8 wave parameters, as it can only be observed measured in the absence of a signal. For this reason, we assume that the noise floor of the a and b waves are each sampled from the same distribution regardless of whether the source on a given port is active. For example, we assume that the noise-floor distributions of a_{11} and a_{12} are identical and independent. We also observed that the noise floor on each port of our VNA appeared to be of the same magnitude, so we assumed that the distributions of the wave parameters for each port were the same. For example, we model the distributions of a_{21} and a_{11} as identical and independent.

In our data, we saw no evidence of frequency correlations. Thus, a model that captures frequency correlations correctly will have several independent variables associated with each frequency point. Typical S-parameter measurements have hundreds of frequency points. It is possible to construct such a model, but it would be computationally intensive to use.

V. S-PARAMETER UNCERTAINTIES

Our uncertainty analysis follows the general procedures of the Microwave Uncertainty Framework [7], which supports both Monte-Carlo and sensitivity analyses. In both analyses, the uncertainty is estimated from a model of the measurement process. Both analyses yielded very similar overall uncertainty estimates, so we focus on the sensitivity analysis for brevity.

Let y be the quantity we wish to measure (one of the S-parameters, for example). Also, let x_i with $i = 1, ..., N$ be independent physical variables that affect the measurement outcome. For example, these independent variables might include measured raw wave parameters or physical characteristics of the calibration standards (like length). In this discussion, the noise is modeled by several independent variables corresponding to the eigenvectors of the covariance matrix. Their nominal values are 0, and their standard uncertainties are their measured standard deviations.

Abstractly, the data analysis process can be modelled by a measurement equation.

$$y = f\left(x_1, x_2, ..., x_N\right) \tag{5}$$

Then, the standard uncertainty of the measured value, δy, can be estimated from the standard uncertainties of all of the independent variables δx_i. The standard equation used for propagation of uncertainties is

$$\delta y = \sqrt{\sum_{i=1}^{N} \left(\frac{\partial f}{\partial x_i} \delta x_i\right)^2}. \tag{6}$$

In practice, the data analysis workflow, which includes a VNA calibration algorithm and detailed physical models of the calibration standards, leads to a measurement function f which is impractical to write down due to its complexity.

The Uncertainty Framework's approach is to repeat the calculation of the result N times, using perturbed values. Then, the final uncertainty is estimated by using a finite difference in place of the derivative.

$$\delta y = \left\{\sum_{i=1}^{N} \left[f\left(x_1, ..., x_i + \delta x_i, ..., x_N\right) - f\left(x_1, ..., x_i, ..., x_N\right)\right]^2\right\}^{(1/2)} \tag{7}$$

One advantage of this approach is that perturbations are then tracked through all of the calculations done to the data, and the overall uncertainty is not evaluated until the end. In this way, the effect of correlations is faithfully represented.

This correlated approach is important for trace noise. For example, as we see in Figure 2, a_{11} and b_{11} have rather large uncertainties (about 0.4 degrees). But these uncertainties are quite correlated, so the uncertainty on $S_{11} = a_{11}/b_{11}$ will be much smaller than either a_{11} or b_{11} (about 0.01 degrees). On the other hand, when doing a wave parameter measurement, the distributions of a_{11} and b_{11} by themselves are relevant.

To illustrate the effect of trace noise and the noise floor, we assigned uncertainties to the corrected S-parameters of

two DUTs. The VNA was calibrated with a multiline thru-reflect-line (MTRL) calibration using the traceable calibration kit described in [3]. For our discussion here, we chose two DUTs with very different S-parameters: a quarter-wave offset-short and a matched load.

Our uncertainty analysis includes both the trace noise and the noise floor. Note that since we are looking at corrected data, the final measurement is affected by not just the noise that was present when the DUT was measured, but also the noise that was present when the calibration standards were measured. For comparison, we also include the systematic uncertainties associated with the geometrical imperfections in the calibration standards described in [3], and the repeatability uncertainty estimated from 4 repeated connections.

In Fig. 3, we see the linear magnitude and phase uncertainty of offset short standard. The systematic uncertainties (labelled "Type B") and repeatability ("Repeat") are the largest uncertainty mechanisms for the phase. Surprisingly, even though trace noise mostly affects phase for the raw data, its effect on the uncertainty is most clear in the linear magnitude of highly reflective devices. We speculate that the true magnitude of the reflection coefficient is very close to unity, and any deviations from unity are caused by non-ideal aspects of measurement equipment, such as noise. Thus, the physical Type B models do not capture observed magnitude variations.

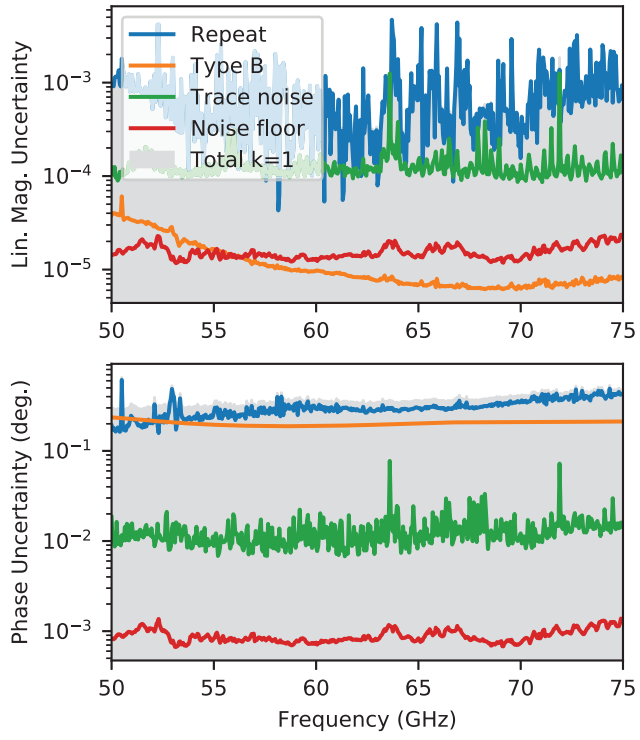

Fig. 3: Uncertainty budget for a corrected measurement of a quarter-wave offset short.

In Fig. 4, we plot the uncertainty budget of a matched load. We plot the data in real and imaginary components, because the phase uncertainty is quite large when the magnitude is close to 0. One might expect that the noise floor is important for a device like the matched load, but we see that the Type B mechanisms are much more important.

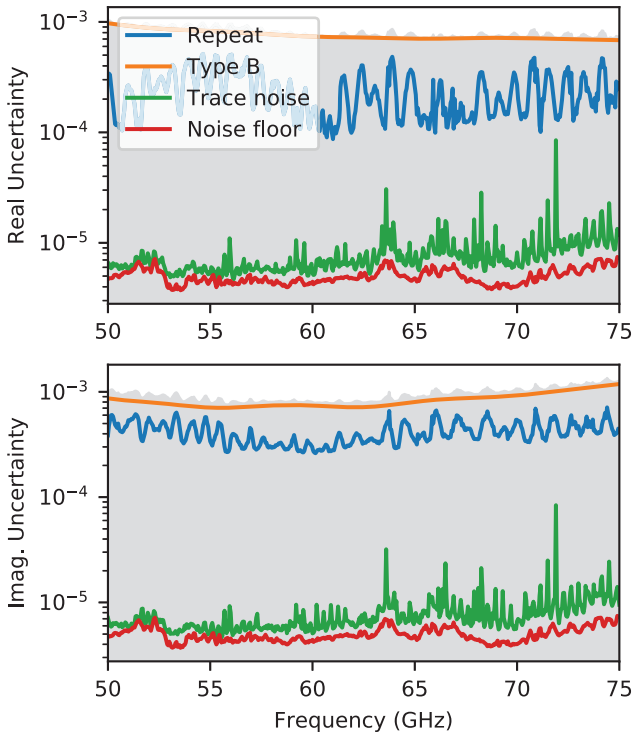

Fig. 4: Uncertainty budget for a corrected measurement of a matched load.

VI. Conclusion

In conclusion, we have characterized the noise floor and trace noise in our WR-15 measurement setup. Our model describes the effect of these two kinds of noise on both wave parameter and S-parameter measurements, and its correlations between measurement ports. More broadly, our primary goal in this paper is to document the development of part of the VNA uncertainty model that we will eventually adopt in our S-parameter and power calibration services. This larger effort requires characterization of several other effects, including VNA drift, VNA nonlinearity, isolation, test port cable stability, and connection repeatability [4]. More broadly, we aim to incorporate this wave-parameter analysis with power and phase calibrations to extend traceability to nonlinear and modulated microwave measurements.

References

[1] A. M. Hagerstrom, A. C. Stelson, J. A. Jargon, and C. J. Long, "Updates to the Traceability of mm-Wave Power Measurements at NIST," *97th ARFTG Microwave Measurement Conference*, Virtual, Jun. 2021.

[2] K. A. Remley, J. A. Gordon, D. Novotny, A. E. Curtin, C. L. Holloway, M. T. Simons, R. D. Horansky, M. S. Allman, D. Senic, M. Becker, J. A. Jargon, P. D. Hale, D. F. Williams, A. Feldman, J. Cheron, R. Chamberlin, C. Gentile, J. Senic, R. Sun, P. B. Papazian, J. Quimby, M. Mujumdar, and N. Golmie, "Measurement Challenges for 5G and Beyond: An Update from the National Institute of Standards and Technology," *IEEE Microwave Magazine*, vol. 18, no. 5, pp. 41–56, 2017.

[3] J. A. Jargon, D. F. Williams, A. C. Stelson, C. J. Long, A. M. Hagerstrom, P. D. Hale, J. R. Stoup, E. S. Stanfield, and W. Ren, "Physical Models and Dimensional Traceability of WR15 Rectangular Waveguide Standards for Determining Systematic Uncertainties of Calibrated Scattering-Parameters," NIST Technical Note 2109, Aug. 2020.

[4] M. Zeier, D. Allal, and R. Judaschke, "EURAMET Calibration Guide No. 12: Guidelines on the Evaluation of Vector Network Analysers (VNA)," *European Association of National Metrology Institutes, Braunschweig*, Version 3.0, Mar. 2018

[5] D. Gu, J. A. Jargon, M. J. Ryan, and A. Hubrechsen, "Influence of Noise on Scattering-Parameter Measurements," *IEEE Transactions on Microwave Theory and Techniques*, vol. 68, no. 11, pp. 4925–4939, 2020.

[6] J. A. Jargon, A. A. Koepke, and P. D. Hale, "Investigating the Effects of IF Bandwidth and Averaging on Calibrated Scattering-Parameter Measurements," *93rd ARFTG Microwave Measurement Conference*, Boston, MA, 2019

[7] "NIST Microwave Uncertainty Framework," 2011. [Online]. Available: http://www.nist.gov/ctl/rf-technology/related-software.cfm